

## San-Zhong-Kui-Jian-Tang, a Traditional Chinese Medicine Prescription, Inhibits the Proliferation of Human Breast Cancer Cell by Blocking Cell Cycle Progression and Inducing Apoptosis

Ya-Ling HSU,<sup>a</sup> Ming-Hong YEN,<sup>b</sup> Po-Lin KUO,<sup>c</sup> Chien-Yu CHO,<sup>d</sup> Yu-Ting HUANG,<sup>c</sup> Chien-Jung TSENG,<sup>d</sup> Ju-Ping LEE,<sup>c</sup> and Chun-Ching LIN<sup>\*,b</sup>

<sup>a</sup> Department of Pharmacy, Chia-Nan University of Pharmacy and Science, Tainan, Taiwan; No. 60, Erh-Jen Road, Sec. 1, Jen-Te, Tainan 717, Taiwan; <sup>b</sup> Faculty of Pharmacy, College of Pharmacy, Kaohsiung Medical University; No. 100, Shin-Chuan 1st Road, Kaohsiung 807, Taiwan; <sup>c</sup> Department of Biotechnology, Chia-Nan University of Pharmacy and Science; No. 60, Erh-Jen Road, Sec. 1, Jen-Te, Tainan 717, Taiwan; and <sup>d</sup> Graduate Institute of Natural Products, Kaohsiung Medical University; No. 100, Shin-Chuan 1st Road, Kaohsiung 807, Taiwan.

Received July 17, 2006; accepted September 19, 2006

**San-Zhong-Kui-Jian-Tang (SZKJT; Japanese name: Sanshu-kaigen-to), a traditional Chinese medicine prescription, has been used for treating patients with various cancers. This study first investigates the anticancer effect of SZKJT in two human breast cancer cell lines, MCF-7 and MDA-MB-231. SZKJT exhibited effective cell growth inhibition by inducing cancer cells to undergo G0/G1 phase arrest and apoptosis. Blockade of cell cycle was associated with increased p21/WAF1 levels, and reduced amounts of cyclinD1, cyclinD2 in a p53-independent manner. SZKJT treatment triggered the mitochondrial apoptotic pathway indicated by changing Bax/Bcl-2 ratios, cytochrome *c* release and caspase-9 activation, but did not act on Fas/Fas ligand pathways and the activation of caspase-8. Further investigation revealed that SZKJT's inhibition of cell growth effect was also evident in a nude mice model. Taken together, our study suggests that the induction of p21/WAF1 and activity of the mitochondrial apoptotic system may participate in the antiproliferative activity of SZKJT in human breast cancer cells.**

**Key words** San-Zhong-Kui-Jian-Tang; breast cancer; cell cycle; apoptosis; p21; mitochondrial

Breast cancer is one of the most common malignancies in women, and is the leading cause of death worldwide for women between the ages of 40 and 55 years in the world.<sup>1)</sup> This pathology is currently controlled by surgery and radiotherapy, and is frequently supported by adjuvant chemo- or hormonotherapies.<sup>2)</sup> However, breast cancer is highly resistant to chemotherapy, and there is still no effective cure for patients with advanced stages of the disease, especially in cases of hormone-independent cancer.<sup>2)</sup> Effective chemopreventive treatment for breast cancer would have an important impact on breast cancer morbidity and mortality. Apoptosis has been characterized as a fundamental cellular activity to maintain the physiological balance of the organism.<sup>3)</sup> It is also involved in immune defense machinery and plays a necessary role as a protective mechanism against carcinogenesis by eliminating damaged cells or abnormal excess cells proliferated owing to various chemical agents' induction.<sup>4,5)</sup> Emerging evidence has demonstrated that the anticancer activities of certain chemotherapeutic agents are involved in the induction of apoptosis, which is regarded as the preferred way to manage cancer.<sup>4,6)</sup>

San-Zhong-Kui-Jian-Tang (SZKJT; Japanese name: Sanshu-kaigen-to), a traditional Chinese medicine prescription, has been used for treating patients with various cancers. In this study, we determined the antiproliferative activity of SZKJT, and examined its effect on cell cycle distribution and apoptosis in the human breast cancer cell lines, MCF-7 and MDA-MB-231. Furthermore, to establish the anticancer mechanism of SZKJT, we assayed the levels of p53, p21/WAF1, Fas/APO-1 receptor, Fas ligand, Bcl-2 family protein and caspases activity, which are strongly associated with the signal transduction pathway of apoptosis and affect

the chemosensitivity of tumor cells to anticancer agents.<sup>7)</sup>

### MATERIALS AND METHODS

**Chemicals and Reagents** Fetal calf serum (FCS), nonessential amino acids, sodium pyruvate, insulin, Dulbecco's modified Eagle's medium (DMEM) and RPMI 1640 were obtained from GIBCO BRL (Gaithersburg, MD, U.S.A.). Dimethyl sulfoxide (DMSO), ribonuclease (RNase) and propidium iodide were purchased from Sigma Chemical Co. (St. Louis, MO, U.S.A.). Nucleosome ELISA, WAF1 ELISA, Fas Ligand, Fas/APO-1 ELISA, and caspase-9, caspase-8 activity assay kits were purchased from Calbiochem (Cambridge, MA, U.S.A.). The antibodies to  $\beta$ -actin, cyclinD1, cyclinD2, cyclinB, Bax, Bak, Bcl-2, and Bcl-X<sub>L</sub> were obtained from Santa Cruz Biotechnology (Santa Cruz, CA, U.S.A.).

**Plant Materials** It was prepared as a lyophilized-dry powder of hot water extracts from 17 species of medical herbs consisting of *Coptis chinensis* FRANCH (5.6 g), *Cimicifuga heracleifolia* KOMAR (8.6 g), *Scutellaria baicalensis* GEORGI (22.9 g), *Gentiana scabra* BUNGE. (14.3 g), *Trichosanthes cucumeroides* (SER.) MAXIM. (14.3 g), *Phellodendron amurense* RUPR. (22.9 g), *Anemarrhena asphodeloides* BUNGE. (14.3 g), *Platycodon grandiflorum* (JACQ.) (14.3 g), *Laminaria japonica* ARESCH. (14.3 g), *Bupleurum chinese* DC. (14.3 g), *Glycyrrhiza uralensis* FISCH. (8.6 g), *Sparganium stoloniferum* BUCCH. (8.6 g), *Curcuma aeruginosa* ROXB (8.6 g), *Forsythia suspense* (THUMB.) VAHL (8.6 g), *Pueraria lobata* OHWI (8.6 g), *Paeonia lactiflora* PALL. (5.6 g) and *Angelica sinensis* (OLIV.) DIELS. (5.6 g). They were purchased from a local herb store. The authenticity of the plant species

\* To whom correspondence should be addressed. e-mail: aalin@ms24.hinet.net

was confirmed by Doctor MH Yen of Graduate Institute of Natural Products, Kaohsiung Medical University, Taiwan. Each recipe (200 g) was decocted three times with 1 l boiling distilled water for 2 h. The decoction was filtered, collected, concentrated, and lyophilized. The average yield obtained for SZKJT was 20.7%.

**Cell Cultures** Breast cancer cell lines MCF-7 (ATCC HTB-22), MDA-MD-231 (ATCC HTB-26), and IMR-90 (ATCC CCL-186) normal lung fibroblast cells and BNL CL.2 (ATCC TIB-73) normal murine liver cells were obtained from the American Type Cell Culture Collection (Manassas, VA, U.S.A.). Normal mammary epithelial cell H184B5F5/M10 was purchased from Bioresource Collection and Research Center (Hsinchu, Taiwan). MCF-7, IMR-90, H184B5F5/M10, and BNL CL.2 cells were cultured in DMEM with nonessential amino acids, 0.1 mM sodium pyruvate, 10  $\mu$ g/ml insulin, and 10% FCS. The MDA-MB-231 cells were cultured in RPMI 1640 (Life Technologies, Inc., Grand Island, NY, U.S.A.) supplemented with 10% FCS and 1% penicillin-streptomycin solution (Life Technologies, Inc.).

**Cell Proliferation Assay (XTT)** Inhibition of cell proliferation by SZKJT was measured by XTT (sodium 3'-[1-(phenylamino-carbonyl)-3,4-tetrazolium]-bis(4-methoxy-6-nitro)benzene-sulfonic acid hydrate) assay. Briefly, cells were plated in 96-well culture plates ( $1 \times 10^4$  cells/well). After 24 h incubation, the cells were treated with SZKJT (0, 100, 200, 300  $\mu$ g/ml) for 48 h. Fifty microliters of XTT test solution, which was prepared by mixing 5 ml of XTT-labeling reagent with 100  $\mu$ l of electron coupling reagent, was then added to each well. After 4 h incubation, absorbance was measured on an ELISA reader (Multiskan EX, Labsystems) at a test wavelength of 492 nm and a reference wavelength of 690 nm. Data were calculated as the percentage of inhibition by the following formula: inhibition % =  $[100 - (\text{ODt}/\text{ODs}) \times 100]\%$ . ODt and ODs indicated the optical density of the test substances and the solvent control, respectively. The concentration of 50% cellular cytotoxicity of cancer cells (IC<sub>50</sub>) of test substances was calculated based on 48 h absorbance values.

**Cell Cycle Analysis** To determine cell cycle distribution analysis,  $5 \times 10^5$  cells were plated in 60 mm dishes and treated with SZKJT (100, 200  $\mu$ g/ml) for 12 h. After treatment, the cells were collected by trypsinization, fixed in 70% ethanol, washed in phosphate-buffered saline (PBS), resuspended in 1 ml of PBS containing 1 mg/ml RNase and 50  $\mu$ g/ml propidium iodide, incubated in the dark for 30 min at room temperature, and analyzed by EPICS flow cytometer. The data were analyzed using Multicycle software (Phoenix Flow Systems, San Diego, CA, U.S.A.).

**Measurement of Apoptosis** Quantitative assessment of apoptosis was analyzed by an Annexin V assay kit (BD Biosciences PharMingen, San Jose, CA, U.S.A.). Briefly, cells grown in 10 cm Petri dishes were harvested with trypsin and washed in PBS. Cells were then resuspended in binding buffer (10 mmol/l HEPES/NaOH (pH 7.4), 140 mmol/l NaCl, 2.5 mmol/l CaCl<sub>2</sub>) and stained with Annexin V-FITC and PI at room temperature for 15 min in the dark. Cells were then analyzed in an EPICS flow cytometer (Coulter Electronics) within 1 h after staining. Data from 10000 cells were collected for each data file. Apoptotic cells were defined as Annexin V-positive, PI-negative cells.

Quantitative assessment of apoptotic cells was also assessed by the terminal deoxynucleotidyl transferase-mediated deoxyuridine triphosphate nick end labeling (TUNEL) method, which examines DNA-strand breaks during apoptosis by using BD ApoAlert™ DNA Fragmentation Assay Kit. Briefly, cells were incubated with 100 and 200  $\mu$ g/ml SZKJT for the indicated times. The cells were trypsinized, fixed with 4% paraformaldehyde, and permeabilized with 0.1% Triton X-100 in 0.1% sodium citrate. After being washed, the cells were incubated with the reaction mixture for 60 min at 37 °C. The stained cells were then analyzed with an EPICS flow cytometer.

**Assaying the Levels of p53, p21/WAF1, Fas/APO-1 and Fas Ligand (mFasL and sFasL)** p53 pan ELISA, WAF1 ELISA, Fas/APO-1 ELISA and Fas Ligand ELISA kits were used to detect p53, p21/WAF1, Fas/APO-1 receptor and FasL. Briefly, cells were treated with 0, 100, and 200  $\mu$ g/ml SZKJT for the indicated times. The samples of cell lysate were placed in 96 well ( $1 \times 10^6$  per well) microtiter plates coated with monoclonal detective antibodies, and were incubated for 1 h (Fas/APO-1), 2 h (p53 or p21/WAF1) or 3 h (Fas ligand) at room temperature. It was necessary to determine the soluble Fas ligand in cell culture supernatant by using Fas Ligand ELISA kit. After removing unbound material by washing with washing buffer (50 mM Tris, 200 mM NaCl, and 0.2% Tween 20), horseradish peroxidase conjugated streptavidin was added to bind to the antibodies. Horseradish peroxidase catalyzed the conversion of a chromogenic substrate (tetramethylbenzidine) to a colored solution, with color intensity proportional to the amount of protein present in the sample. The absorbance of each well was measured at 450 nm, and concentrations of p53, p21/WAF1, Fas/APO-1 and Fas L were determined by interpolating from standard curves obtained with known concentrations of standard proteins.

**Assay for Caspase-8 and -9 Activities** The assay is based on the ability of the active enzyme to cleave the chromophore from the enzyme substrate: Ac-IETD-pNA (Ac-Ile-Glu-Thr-Asp-pNA) for caspase-8, and LEHD-pNA (Ac-Leu-Glu-His-Asp-pNA) for caspase-9. Cell lysates were incubated with peptide substrate in assay buffer (100 mM NaCl, 50 mM HEPES, 10 mM dithiothreitol, 1 mM EDTA, 10% glycerol, 0.1% CHAPS, pH 7.4) for 2 h at 37 °C. The release of p-nitroaniline was monitored at 405 nm. Results are represented as the percentage of change of activity compared to the untreated control.

**Immunoblot Assay** Cells were treated with 200  $\mu$ g/ml SZKJT for specified intervals of time. Mitochondrial and cytoplasmic fractions were separated using Cytochrome c Releasing Apoptosis Assay Kit (BioVision, California, U.S.A.). For immunoblotting, the cells were lysed on ice for 40 min in a solution containing 50 mM Tris, 1% Triton X-100, 0.1% SDS, 150 mM NaCl, 2 mM Na<sub>3</sub>VO<sub>4</sub>, 2 mM EGTA, 12 mM  $\beta$ -glycerolphosphate, 10 mM NaF, 16  $\mu$ g/ml benzamidine hydrochloride, 10  $\mu$ g/ml phenanthroline, 10  $\mu$ g/ml aprotinin, 10  $\mu$ g/ml leupeptin, 10  $\mu$ g/ml pepstatin, and 1 mM phenylmethylsulfonyl fluoride. The cell lysate was centrifuged at 14000  $\times$ g for 15 min, and the supernatant fraction was collected for immunoblotting. Equivalent amounts of protein were resolved by SDS-PAGE (10–12%) and transferred to PVDF membranes. After blocking for 1 h in 5% nonfat dry

milk in Tris-buffered saline, the membrane was incubated with the desired primary antibody for 1–16 h. The membrane was then treated with appropriate peroxidase-conjugated secondary antibody, and the immunoreactive proteins were detected using an enhanced chemiluminescence kit (Amersham, U.S.A.) according to the manufacturer's instructions.

**In Vivo Tumor Xenograft Study** Female nude mice [6 weeks old; BALB/cA-nu (nu/nu)] were purchased from National Science Council Animal Center (Taipei, Taiwan) and maintained in pathogen-free conditions. MDA-MB-231 cells were injected subcutaneously into the flanks of nude mice ( $5 \times 10^6$  cells in  $200 \mu\text{l}$ ). Tumors were allowed to develop for ca. 30 d until they reached ca.  $75 \text{ mm}^3$ , when treatment was initiated. Twenty mice were randomly divided into two groups. SZKJT was dissolved in sterilized distilled water, and a nude mouse received  $1000 \text{ mg/kg}$  of SZKJT in  $0.5 \text{ ml}$  of water through a naso-gastric tube (twice a day). The control group was treated with an equal volume of normal saline. After transplantation, tumor size was measured using calipers and tumor volume was estimated according to the formula: tumor volume ( $\text{mm}^3$ ) =  $L \times W^2/2$ , where  $L$  is the length and  $W$  is the width.

**Statistical Analysis** Data were expressed as means  $\pm$

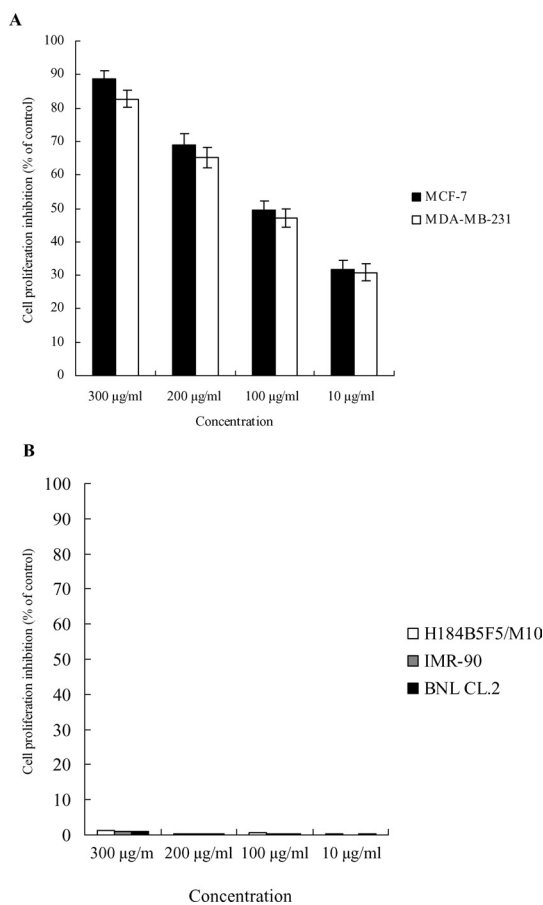


Fig. 1. Effect of SZKJT on the Proliferation Inhibition in MCF-7 and MDA-MB-231 Cells

The effect of SZKJT in breast cancer cells (A) and various normal cells (B). Cells were seeded into 96-well plates ( $10^4$  cells/well) and allowed to adhere overnight. The next day, the cells were incubated with vehicle (0.1% DMSO) and different concentrations of SZKJT for 48 h. Cell proliferation was determined by XTT assay. Results are expressed as percent cell proliferation relative to the proliferation of control. Each value is the mean  $\pm$  S.D. of three determinations.

S.D. Statistical comparisons of the results were made using analysis of variance (ANOVA). Significant differences ( $p < 0.05$ ) between the means of control and SZKJT-treated cells were analyzed by Dunnett's test.

## RESULTS

**Effect of SZKJT on Cell Proliferation in MCF-7 and MDA-MB-231 Cell Lines** As shown in Fig. 1A, SZKJT inhibited cell growth in two human breast cancer cell lines in a concentration-dependent manner, with MCF-7 being more sensitive to SZKJT-induced cell growth inhibition than MDA-MB-231. The  $\text{IC}_{50}$  values of SZKJT were  $103.2 \mu\text{g/ml}$  for MCF-7 and  $116.2 \mu\text{g/ml}$  MDA-MB-231. Interestingly, the proliferation inhibitory effect of SZKJT on H184B5F5/M10 normal mammary epithelial cells, IMR-90 normal lung fibroblast cells, and BNL CL.2 normal murine liver cells was not significant at the same concentrations as on tumor cells (Fig. 1B).

**Effect of SZKJT on Cell Cycle Distribution in MCF-7 and MDA-MB-231 Cell Lines** To examine the mechanism responsible for SZKJT-mediated cell growth inhibition, cell cycle distribution was evaluated using flow cytometric analysis. The results showed that treating cells with SZKJT caused a significant inhibition of cell cycle progression in both MCF-7 and MDA-MB-231 cells at 12 h and 24 h (Figs. 2A, B), resulting in a clear increase of the percentage of cells in

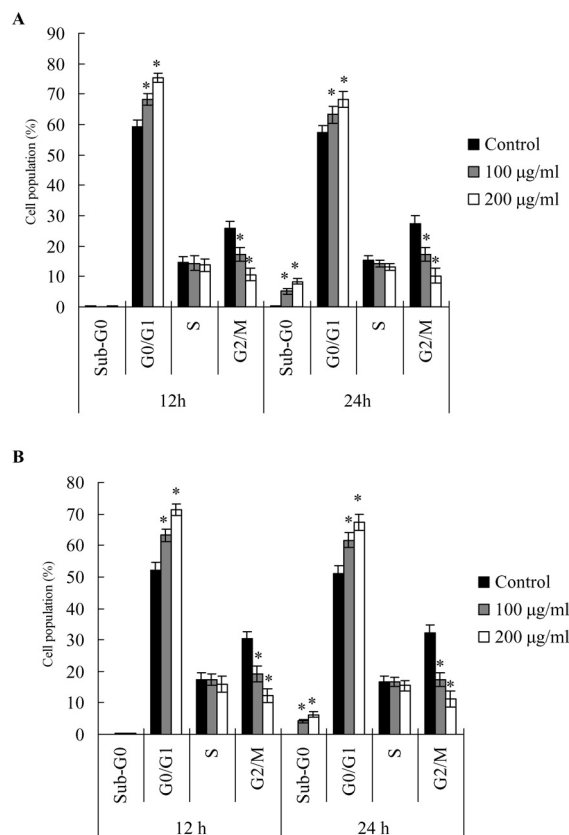


Fig. 2. The Distribution of Cell Cycle in SZKJT Treated MCF-7 (A) and MDA-MB-231 Cells (B)

Cells were treated with vehicle (0.1% DMSO), 100 and  $200 \mu\text{g/ml}$  SZKJT for 12 and 24 h. The distribution of cell cycle was assessed by flow cytometry. Each value is the mean  $\pm$  S.D. of three determinations. The asterisk indicates a significant difference between control and SZKJT-treated cells as analyzed by Dunnett's test,  $p < 0.05$ .

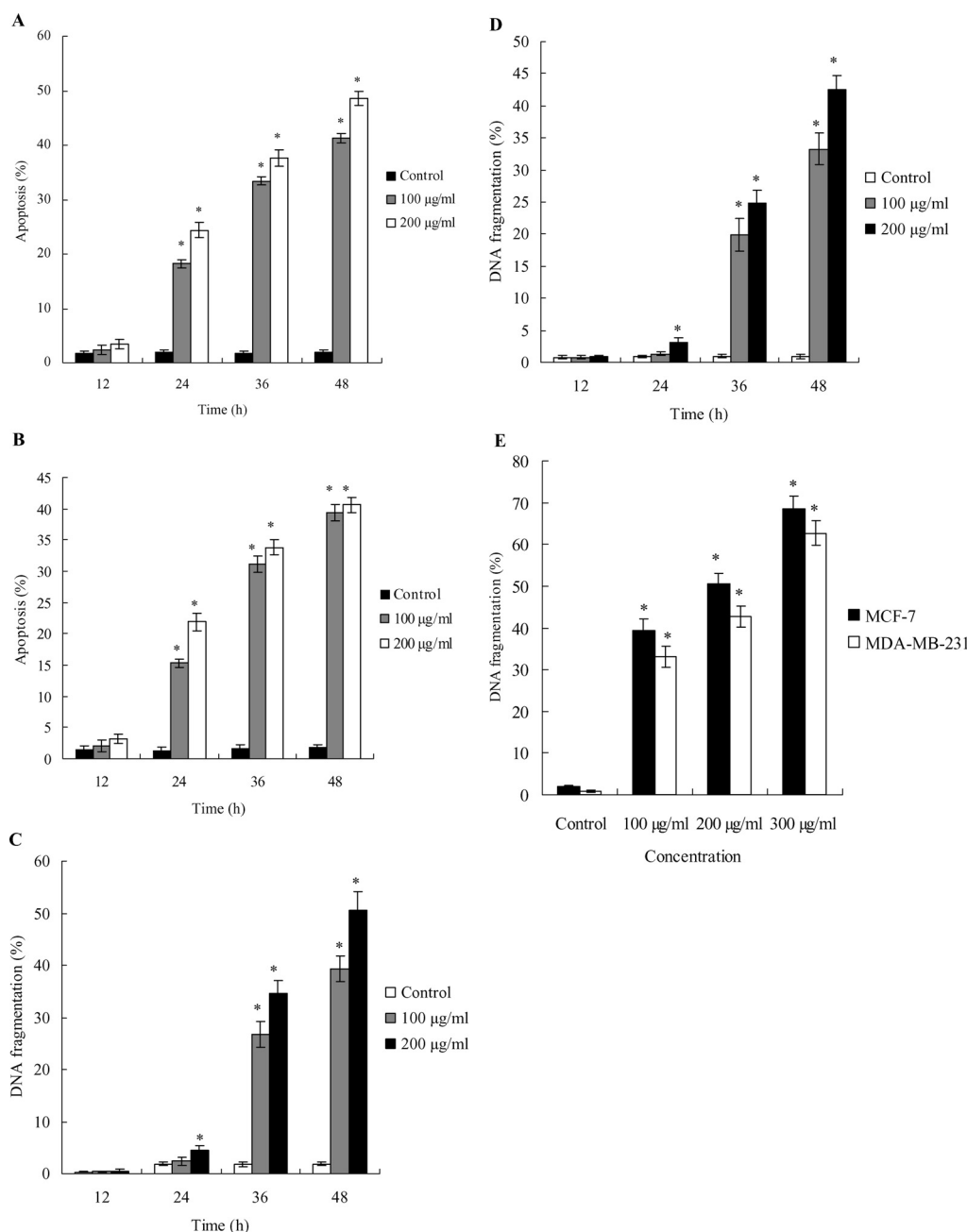


Fig. 3. The Induction of Apoptosis of MCF-7 and MDA-MB-231 by SZKJT Treatment

The quantitation of apoptosis in MCF-7 (A) and MDA-MB-231 (B) cells by Annexin V-FITC/PI staining. The analysis of apoptosis in MCF-7 (C) and MDA-MB-231 (D) cells by using TUNEL method. (E) The effect of SZKJT on apoptosis in a dose-dependent manner. Cells were treated with vehicle alone (0.1% DMSO) and various concentration of SZKJT for the indicated time. The phosphatidylserine translocation and cytoplasmic oligonucleosome of SZKJT treated cells was estimated by Annexin V assay. Each value is the mean  $\pm$  S.D. of three determinations. The asterisk indicates a significant difference between control and SZKJT-treated cells as analyzed by Dunnett's test,  $p < 0.05$ .

the G0/G1 phase when compared with the control.

**SZKJT Induced Apoptosis in Both MCF-7 and MDA-MB-231** A quantitative evaluation of apoptosis was sought using an Annexin V-FITC dye to detect the translocation of phosphatidylserine from the inner (cytoplasmic) leaflet of the plasma membrane to the outer (cell surface). Compared with vehicle-treated cells, 200  $\mu\text{g/ml}$  SZKJT induced 48.6% and 40.6% of apoptotic cells in MCF-7 and MDA-MB-231 at 48 h, respectively (Figs. 3A, B). Additionally, a quantitative evaluation was sought using TUNEL to detect the amount of DNA fragmentation. Compared with vehicle-treated cells, 200  $\mu\text{g/ml}$  SZKJT induced 50.6% and 42.6% of cytoplasmic

oligonucleosome in MCF-7 and MDA-MB-231 at 48 h, respectively (Figs. 3C, D). The proapoptotic effect of SZKJT was also observed in a dose-dependent manner after 48 h treatment (Fig. 3E).

**Effect of SZKJT on Cell Cycle-Related Molecules** We next examined the effect of SZKJT on cell cycle-regulatory molecules, including p53, p21/WAF1, cyclinD1, cyclinD2, and cyclinB. Previous reports have indicated that MCF-7 cells have a normal tumor suppression gene, p53, whereas in MDA-MB-231 cells the major protein of the p53 gene has mutated and is accompanied by the absence of p53 function.<sup>8,9</sup> As shown in Fig. 4A, SZKJT failed to affect the ex-

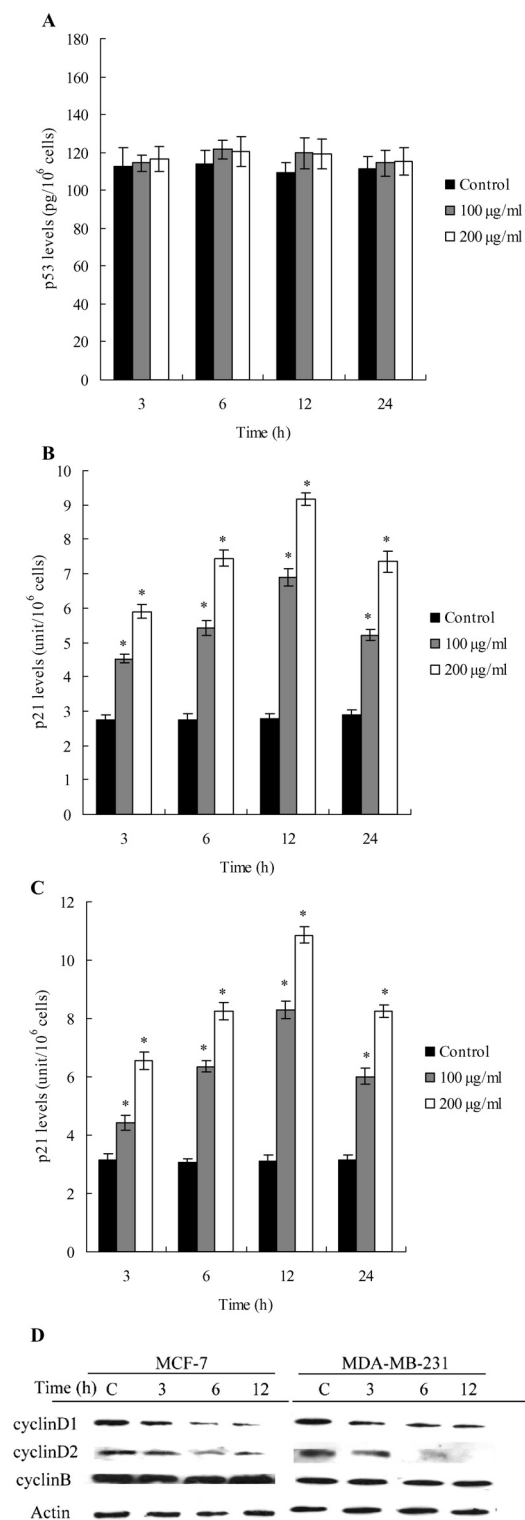


Fig. 4. Effects of SZKJT on the Expressions of Cell Cycle-Related Proteins

The level of p53 in MCF-7 cells (A). The amount of p21/WAF1 in MCF-7 (B) and MDA-MB-231 (C) cells. The expressions of cyclinD1, cyclinD2, and cyclinB in SZKJT-treated cells (D). Cells were treated with vehicle (0.1% DMSO), 100 and 200  $\mu$ g/ml SZKJT for the indicated time. The level of p53 and p21/WAF1 protein was measured by p53 pan and WAF1 ELISA kit. The amount of cyclinD1, cyclinD2, and cyclinB was assessed by Western blot assay. Each value is the mean  $\pm$  S.D. of three determinations. The asterisk indicates a significant difference between control and SZKJT-treated cells as analyzed by Dunnett's test,  $p < 0.05$ .

pression of p53 at any of the examined time points in MCF-7 cells, but increased the expression of p21/WAF1 in both MCF-7 and MDA-MB-231 cells (Figs. 4B, C). Furthermore, SZKJT treatment of the cells resulted in a time-dependent decrease in the protein expression of cyclinD1, cyclinD2 in both MCF-7 and MDA-MB-231 cells (Fig. 4D).

**Fas/Fas Ligand Is Not Involved in SZKJT-Mediated Apoptosis** To establish the sequence of events occurring during SZKJT-induced apoptosis, we measured some of the molecular activity of the death receptor apoptotic pathway, including Fas/APO-1 receptor and its two ligands, mFas ligand and sFas ligand. However, treatment of either of these two cell lines with 100 or 200  $\mu$ g/ml SZKJT failed to affect the levels of these proteins at any of the examined time points, including Fas/APO-1, mFas ligand and sFas ligand (data not shown). In addition, SZKJT also failed to affect the activation of caspase-8 in both MCF-7 and MDA-MB-231 cells (data not shown).

**SZKJT Induces the Execution of Apoptosis through Activation of the Mitochondrial Pathway** To investigate the mitochondrial apoptotic events involved in SZKJT-induced apoptosis, we first analyzed the changes in the levels of pro-apoptotic protein Bax and Bak, and anti-apoptotic protein Bcl-2. Western blot analysis showed that treatment of MCF-7 and MDA-MB-231 cells with SZKJT increased Bax and Bak protein levels (Fig. 5A). In contrast, SZKJT decreased Bcl-2, which led to an increase in the proapoptotic/antiapoptotic Bcl-2 ratio (Fig. 5A).

Cytosolic extracts were prepared under conditions to preserve the mitochondria, and cytosolic cytochrome *c* protein levels were measured by immunoblotting analysis. Figure 5B shows that the cytosolic fraction from untreated MCF-7 and MDA-MB-231 cells contained no detectable amounts of cytochrome *c*, whereas it did become detectable after 12 h of 200  $\mu$ g/ml SZKJT treatment in both MCF-7 and MDA-MB-231 cells.

Hallmarks of the apoptotic process include the activation of cysteine proteases, which represent both initiators and executors of cell death. Upstream caspase-9 activities increased significantly as shown by the observation that treatment with SZKJT increased caspase-9 activity in both MCF-7 and MDA-MB-231 cells. This is consistent with the release of cytochrome *c* into the cytosol (Figs. 5C, D).

To verify the relation of apoptosis and cytotoxicity in SZKJT-treated breast cancer cells, we used pan-caspase inhibitor to block caspase activity in both cell lines and determine whether the cell proliferation inhibition was changed after SZKJT treatment. Blocked of caspases activation resulted in a completely decreased in SZKJT-mediated proliferation inhibition in both cell lines (Fig. 5E), suggesting that SZKJT inhibits cell proliferation inhibition by apoptosis induction.

**SZKJT Inhibits Tumor Growth in Nude Mice** To determine whether SZKJT inhibits tumor growth *in vivo*, equal numbers of MDA-MB-231 cells were injected subcutaneously into both flanks of the nude mice. Tumor growth inhibition was most evident in mice treated with SZKJT at 1000 mg/kg, (twice day) where *ca.* 40% reductions in tumor size were observed, in contrast with mice treated with the vehicle (Figs. 6A, B). No sign of toxicity, as judged by parallel monitoring body weight, was observed in SZKJT-treated

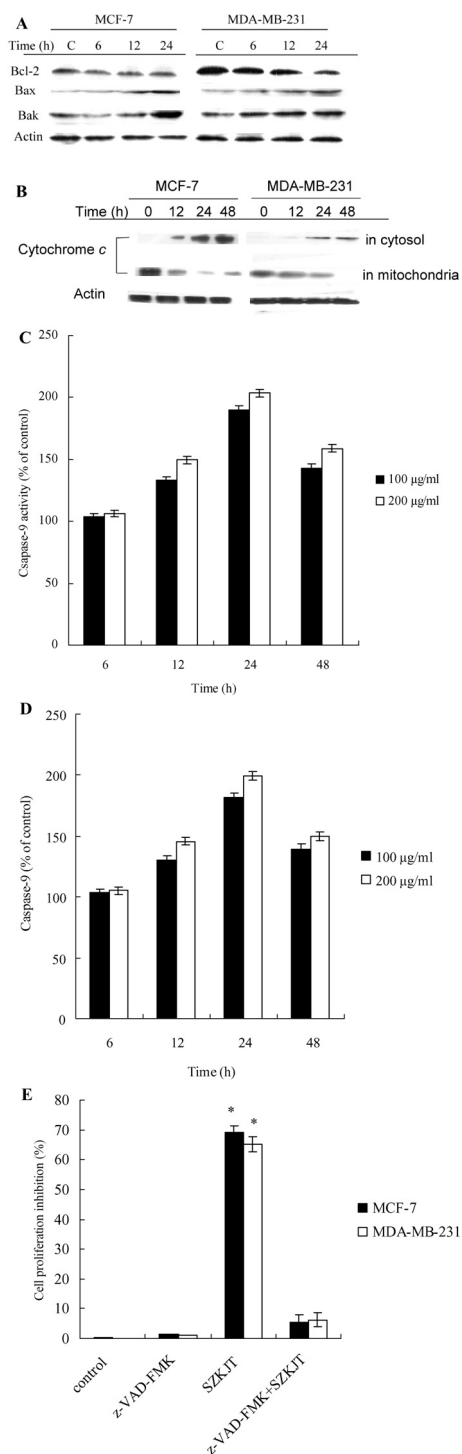


Fig. 5. SZKJT Induced Apoptosis through the Initiation of the Mitochondrial Pathway

(A) The effect of SZKJT on Bcl-2 family proteins. (B) The release of cytochrome *c* in MCF-7 and MDA-MB-231 cells. The activation of caspase-9 in MCF-7 (C) and MDA-MB-231 (D) cells. (E) The effect of pan-caspase inhibitor on SZKJT-mediated cell proliferation inhibition. For (A) and (B), cells were treated with 200 µg/ml SZKJT for the indicated time. The extraction of cytoplasm and mitochondria were separated from cell pellet by lysis buffer and centrifugation. Western blotting analysis assessed the protein expressions. For (C) to (D), the activity of caspase-9 was assessed by caspase-9 activity assay kit. For (E), cells were treated z-VAD-FMK (20 µM) for 1 h, and then incubated with SZKJT (200 µg/ml) for 48 h. The cell proliferation was assessed by XTT assay. Each value is the mean ± S.D. of three determinations. The asterisk indicates a significant difference between control and SZKJT-treated cells as analyzed by Dunnett's test,  $p < 0.05$ .

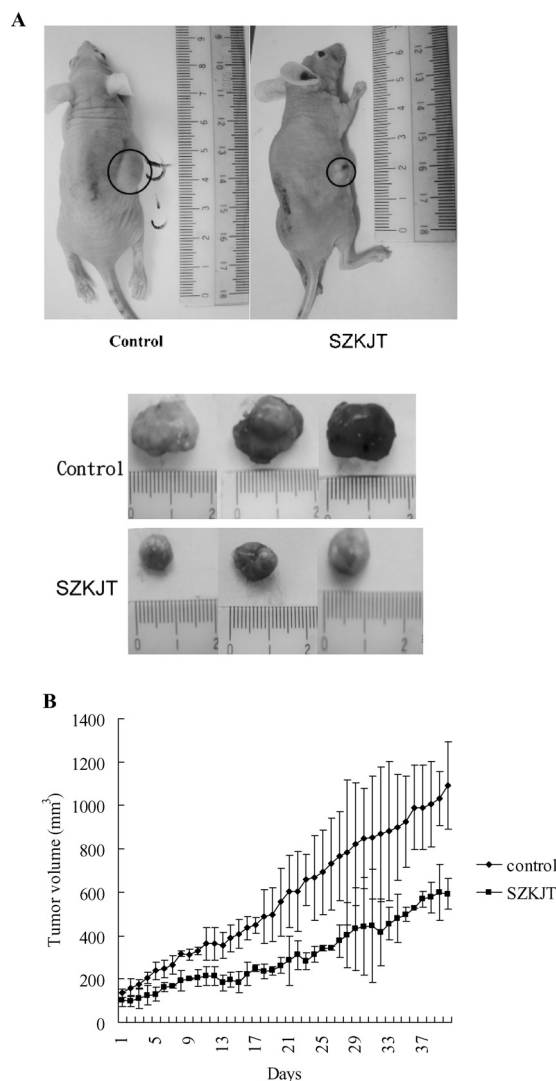


Fig. 6. SZKJT Inhibits Growth in Nude Mice

(A) Representative tumor-bearing nude mice and tumors from the control and SZKJT-treated groups. (B) Mean of tumor volume measured at the indicated number of days after implant. Animals bearing pre-established tumors ( $n = 15$  per group) were dosed daily for 40 d with *p.o.* of SZKJT (1000 mg/kg, twice a day) or vehicle. During the 40-d treatment, tumor volumes were estimated using measurements taken from external calipers (mm<sup>3</sup>).

mice.

## DISCUSSION

Breast cancer is the most common neoplasm in human in both developed and developing countries.<sup>10,11</sup> In our study, we have found that SZKJT effectively inhibits tumor cell growth *in vitro*, concomitant with induction of cell cycle arrest and apoptosis, and inhibits tumor cell growth in nude mice. Furthermore, because SZKJT do not exhibit any significant toxicity on various normal cells, this suggests that SZKJT possesses selectivity between normal and cancer cells. This selection of SZKJT to cancer cells may be related to the different genomic stability between cancer and normal cells.<sup>12</sup>

Eukaryotic cell cycle progression involves sequential activation of Cdks, whose activation is dependent upon their association with cyclins.<sup>13</sup> A complex formed by the associa-

tion of Cdc4/6 and cyclin D1/D2 plays a major role at entry into S phase.<sup>14,15</sup> Cell cycle progression is also regulated by the relative balance between the cellular concentration of cyclin-dependent kinase inhibitors (CKIs), such as members of the cyclin-dependent kinase-interacting protein/cyclin-dependent kinase inhibitory protein (CIP/KIP) and inhibitor of cyclin-dependent kinase (INK) families, and that of cyclin-CDK complexes. The Cip/Kip family, including p21/WAF1, and p27/KIP, bind to cyclin-CDK complexes and prevent kinase activation and subsequently blocks the progression of cell cycle at G0/G1 or G2/M phase.<sup>15,16</sup> In our result, we found that SZKJT treatment not only causes a significant increase in the expression of p21 both in MCF-7 and MDA-MB-231 cells, but also decreases the expressions of cyclinD1, and cyclinD2. Thus, it is reasonable to postulate that SZKJT treatment may cause cell cycle arrest by regulating the expressions of G0/G1 regulating proteins.

Two major distinct apoptotic pathways have been described for mammalian cells. One involves caspase-8, which is recruited by the adapter molecule Fas/APO-1 associated death domain protein to death receptor upon Fas ligand binding.<sup>3,17</sup> We did not observe any alteration of either Fas/APO-1 or Fas ligand (mFas ligand and sFas ligand) expression or caspase-8 activation in SZKJT-treated MCF-7 and MDA-MB-231 cells. On the other hand, SZKJT treatment resulted in a significant increase of Bax and Bak expression, and decreased the amount of Bcl-2, suggesting that changes in the ratio of proapoptotic and antiapoptotic Bcl-2 family proteins might contribute to the apoptosis-promotion activity of SZKJT. These regulatory effects of SZKJT on the Bcl-2 family are correlated with the release of cytochrome *c* from the mitochondria into the cytoplasm and the activation of caspase-9.

In this study, we concluded that the molecular mechanisms during SZKJT-mediated growth inhibition in MCF-7 and MDA-MB-231 cells involved the (1) induction of apoptosis, (2) blockade of cell cycle progression by regulating cell cycle-related factor, (3) trigger of mitochondrial pathway, (4)

modulation of Bcl-2 family protein, and (5) inhibition of cancer growth in nude mice. We demonstrated that SZKJT may be a promising chemotherapy agent for treating breast cancer.

**Acknowledgements** This study was supported by Committee on Chinese Medicine and Pharmacy of Taiwan (CCMP94-RD-045).

## REFERENCES

- 1) Baselga J., Mendelsohn J., *Breast Cancer Res. Treat.*, **29**, 127—138 (1994).
- 2) Bange J., Zwick E., Ullrich A., *Nat. Med.*, **7**, 548—552 (2001).
- 3) Hengartner M. O., *Nature (London)*, **407**, 770—776 (2000).
- 4) Fesik S. W., *Nat. Rev. Cancer*, **5**, 876—885 (2005).
- 5) Li Y., Ahmed F., Ali S., Philip P. A., Kucuk O., Sarkar F. H., *Cancer Res.*, **65**, 6934—6942 (2005).
- 6) Hsu Y. L., Kuo P. L., Lin L. T., Lin C. C., *J. Pharmacol. Exp. Ther.*, **313**, 333—344 (2005).
- 7) Krajewski S., Krajewska M., Turner B. C., Pratt C., Howard B., Zapata J. M., Frenkel V., Robertson S., Ionov Y., Yamamoto H., Perucho M., Takayama S., Reed J. C., *Endocr. Relat. Cancer*, **6**, 29—40 (1999).
- 8) Amellem O., Stokke T., Sandvik J. A., Smedshammer L., Pettersen E. O., *Exp. Cell Res.*, **232**, 361—370 (1997).
- 9) Negrini M., Sabbioni S., Haldar S., Possati L., Castagnoli A., Corallini A., Barbanti-Brodano G., Croce C. M., *Cancer Res.*, **54**, 1818—1824 (1994).
- 10) Houssami N., Cuzick J., Dixon J. M., *Med. J. Aust.*, **184**, 230—234 (2006).
- 11) Singletary S. E., Connolly J. L., *CA Cancer J. Clin.*, **56**, 37—47 (2006).
- 12) Yang C. H., Craise L. M., *Adv. Space Res.*, **14**, 115—120 (1994).
- 13) Sancar A., Lindsey-Boltz L. A., Unsal-Kacmaz K., Linn S., *Annu. Rev. Biochem.*, **73**, 39—85 (2004).
- 14) Liu Y., Lu C., Shen Q., Munoz-Medellin D., Kim H., Brown P. H., *Oncogene*, **23**, 8238—8246 (2004).
- 15) Schwartz G. K., Shah M. A., *J. Clin. Oncol.*, **23**, 9408—9421 (2005).
- 16) Frey M. R., Saxon M. L., Zhao X., Rollins A., Evans S. S., Black J. D., *J. Biol. Chem.*, **272**, 9424—9435 (1997).
- 17) Chopin V., Slomianny C., Hondermarck H., Le Bourhis X., *Exp. Cell Res.*, **298**, 560—573 (2004).